Environmental Pollution 340 (2024) 122812

Contents lists available at ScienceDirect

Environmental Pollution

journal homepage: www.elsevier.com/locate/envpol

Characterizing accumulation and negative effects of aerosol particles on the leaves of urban trees☆

Siqi Chen[a], Hua Yu[a,*], Liang Xu[b], Fangmin Fei[a], Yaobin Song[a], Ming Dong[a], Weijun Li[c]

[a] Key Laboratory of Hangzhou City for Ecosystem Protection and Restoration, College of Life and Environmental Sciences, Hangzhou Normal University, Hangzhou, 311121, China
[b] College of Sciences, China Jiliang University, Hangzhou, 310018, China
[c] Department of Atmospheric Science, School of Earth Sciences, Zhejiang University, Hangzhou, 310027, China

ARTICLE INFO

Keywords:
Aerosol particle
Leaf functional trait
Particulate matter pollution
Particle retention efficiency
Urban greening trees

ABSTRACT

Urban vegetation can alleviate particulate matter (PM) pollution. Many studies examined the PM retention efficiencies of different plant species, but the PM changes retained on leaf surfaces and their effects on plant leaves have rarely been explored. In this study, two common urban greening tree species of the Yangtze River Delta (*i.e.*, *Broussonetia papyrifera* and *Osmanthus fragrans*) were selected to explore the compositions of retained PM and assess their adverse impacts on leaf functional traits. Compared with *B. papyrifera*, *O. fragrans* with higher wax content was more efficient in particle accumulation, specifically fine ($\Phi \leq 2.5$ μm) and coarse ($2.5 < \Phi \leq 10$ μm) particles. The number density and mass concentration of retained PM on plant leaves tended to increase during the accumulation period. Plant species and accumulation time were two major factors to influence particle retention efficiency. Interestingly, the accumulation of particle retention influenced leaf functional traits, such as photosynthesis rate, stomatal conductance, and transpiration rate. The microscopic observations of PM on leaves confirmed that the toxic components of the retained particles potentially caused leaf injury and stomatal damage. Therefore, the acclimation mechanisms of plants responding to the retained urban aerosols should be paid attention in highly polluted areas.

1. Introduction

In recent decades, atmospheric particulate matter (PM) has become a leading environmental problem that has adverse effects on public health, climate change, and the ecosystem balance (Grantz et al., 2003; Li et al., 2017). For example, as the main source of PM pollution in the urban atmosphere, exhaust emissions from vehicle traffic contain harmful components, such as toxic metals and polycyclic aromatic hydrocarbons (Alves et al., 2018; Konczak et al., 2021; Piscitello et al., 2021). Particulate pollution is a major environmental hazard to human health (Qi et al., 2022), and long-term exposure to PM can cause cardiovascular, cerebrovascular and respiratory diseases, as well as mortality (Qi et al., 2022). In particular, pollution from fine PM, referred to as $PM_{2.5}$ (with aerodynamic diameter $\Phi \leq 2.5$ μm), resulted in 4.14 million deaths worldwide in 2019, accounting for 62% of all air pollution-attributable deaths (Health Effects Institute, 2020). Moreover, PM can also negatively affect photosynthesis in plants, reducing their productivity (Popek et al., 2018).

Recently, the mitigation of particulate pollution has received an increasing attention (Barwise and Kumar, 2020; Pace et al., 2021; Targino et al., 2019). Plants have a vast leaf area and can act as a natural sink for PM (Rai, 2016). The complex microstructure of the leaf surface is capable of effectively retaining PM and reducing the concentration of particles in the atmosphere (Baldacchini et al., 2017; Sgrigna et al., 2020; Zhang et al., 2021). For example, Nemitz et al. (2020) discovered that vegetation was estimated to reduce $PM_{2.5}$ concentrations by 10% in the UK; Fares et al. (2020) estimated the total annual removal of PM_{10} (with aerodynamic diameter $\Phi \leq 10$ μm) by vegetation to be 8–8.4 kg hm^{-2} in the urban parks of Italy; Cao et al. (2022) reported that *Cedrus deodara* retained PM at a rate of 11.9 $t\ km^{-2}$ canopy yr^{-1} in China. These studies indicate the great potential of plants in the control of PM pollution.

There are numerous factors related to the particle retention capacity of plants, such as plant characteristics, particle properties, and

☆ This paper has been recommended for acceptance by Admir Créso Targino.

* Corresponding author.
E-mail address: huayu@hznu.edu.cn (H. Yu).

https://doi.org/10.1016/j.envpol.2023.122812
Received 20 April 2023; Received in revised form 10 October 2023; Accepted 25 October 2023
Available online 27 October 2023

meteorological conditions (Chen et al., 2022). Previous studies have reported that multiple leaf functional traits (e.g., trichomes, stomata, grooves, and protrusions) can influence the PM retention efficiency (Gao et al., 2021; Gao et al., 2022; He et al., 2020; Li et al., 2021). However, there are significant differences in the removal efficiency of PM by different plant species or even the same species in different regions (Li et al., 2019). In general, plants growing in areas with higher levels of particulate pollution have more PM trapped on their leaf surfaces (Lu et al., 2018). For example, the leaves of plants growing near roads retained more PM than those growing on a campus (Lu et al., 2018). In addition, both the settling and resuspension of atmospheric PM are affected by wind speed (Janhäll, 2015). As wind speed increases, its effect on the amount of PM on a leaf surface also increases, promoting suspension and reducing the duration of contact between atmospheric PM and the leaf (Beckett et al., 2000). When the wind speed is sufficiently high, it can shake and invert leaves, resulting in PM falling from the leaf surface under the influence of gravity (Xie et al., 2018). Popek et al. (2019) considered that the PM changes on leaves were mostly related to rain but lesser by wind. Indeed, precipitation events can remove accumulated PM from a leaf surface and restore the particulate retention capacity of plant leaves (Xu et al., 2017; Zhang et al., 2019).

Recently, different models have been employed to evaluate overall particle removal by vegetation, and these models include i-tree Eco model (Pace et al., 2021) and the AIRTEE model (Fares et al., 2020). However, these models adopt the same deposition velocities and resuspension rates for all plant species, which cover the differences of the removal efficiency of different plants. Moreover, the PM retention efficiency of plant leaves varies depending on weather conditions and accumulation duration. Once particle accumulation on leaves has reached saturation, the removal efficiency of plants will decline accordingly (Zhou et al., 2020). However, the clear trend of PM retention by different plants in response to accumulation time is still unclear in urban areas.

Atmospheric particles retained on leaf surfaces can have an adverse impact on plant growth and development (Banerjee et al., 2022). For example, particle accumulation increases leaf temperature, degrades epicuticular wax, inhibits transpiration and photosynthesis of the affected plants (Burkhardt and Pariyar, 2014; Konczak et al., 2021; Popek et al., 2018), and consequently reduces their biomass and productivity (Rai, 2016). Moreover, fine particles not only stay on leaf surfaces but also enter through stomatal openings or trichome pathways of plants (Gao et al., 2021; Gao et al., 2022). As a result, heavy metals, polycyclic aromatic hydrocarbons, and other toxic components of particles disturb the normal physiological and biochemical reactions of plants (Huang et al., 2023; Rai, 2016). Therefore, it is necessary to understand the impact of particle retention and the tolerance of urban plants to PM pollution.

This study was designed to investigate the dynamic changes in particle retention and assess its potential effects on plants during different accumulation periods. Two common urban greening tree species of the Yangtze River Delta (*Broussonetia papyrifera* and *Osmanthus fragrans*) were selected for the study, and the relations between leaf functional traits and particle characteristics were determined. This study aimed to (1) explore the major leaf functional traits closely associated with particle retention, (2) analyze the composition characteristics of deposited particles with different accumulation periods, and (3) investigate the changes in leaf functional traits responding to particle accumulation. This study is helpful for understanding the potential impacts of deposited particles on plant leaves and the physiological responses of plants to particulate pollution.

2. Materials and methods

2.1. Sampling site and studied species

The sampling site is located on the Cangqian Campus of Hangzhou Normal University, Hangzhou city, China (30°17′24″ N, 120°0′29″ E), which has a subtropical monsoon climate, with a cool and dry winter, and a hot and humid summer, with mostly evergreen broad-leaved plants. In 2021, the rainfall, mean air temperature and relative humidity in Hangzhou were 1936.8 mm, 18.8 °C and 71%, respectively (http://www.stats.gov.cn/sj/ndsj/2022/indexch.htm). As a typical urban area, the sampling site is close to main roads, there is no industrial activity in the area, and air pollution is mainly from exhaust emissions of vehicles (Yuan et al., 2021).

Table 1
Characteristics of the studied trees.

Species	Families	Growth forms	Leaf traits	Leaf characteristics
Broussonetia papyrifera	Moraceae	Deciduous broadleaved tree	Papery	Rough surface, sparsely hispid, abaxial densely tomentose.
Osmanthus fragrans	Oleaceae	Evergreen broadleaved tree	Leathery	Glabrous surface, abaxial rough.

In this study, two widely distributed trees in the Yangtze River Delta, the deciduous broadleaved tree (*Broussonetia papyrifera*) and evergreen broadleaved tree (*Osmanthus fragrans*), were selected as the studied objects, and they have different leaf features (Table 1). For instance, the leaves of *B. papyrifera* are papery with minimal wax, while the leaves of *O. fragrans* are leathery and covered with a thick waxy layer.

2.2. Sample collections and treatments

At the beginning of the experiment, a clean and soft brush was used to remove all the visible dust particles on both surfaces of plant leaves to prevent any damage to the leaf tissues. To ensure enough samples, we brushed 100 leaves of each species and marked the petioles of all brushed leaves with labeling paper that did not affect the leaves. Sample collections of tree leaves were conducted between 9:00 and 11:00 a.m. from December 27, 2021 to January 8, 2022, on cool and sunny winter days, under moderate PM pollution. Leaf samples were collected every four days with the particle retention and accumulation treatments of 0 day, 4 days, 8 days, and 12 days.

The leaf samples were randomly collected from a height between 1.5 and 2 m. Four leaves were sampled from each tree, with five replications, and a total of 20 leaf samples per plant species were collected each day. The leaf samples were placed in labeled petri dishes and immediately taken into the laboratory. The leaf samples were dried at 60 °C for 24 h and then weighed. Subsequently, the samples were put in sample chambers at a temperature of 24 °C and a relative humidity ranging from 35% to 65%, and they were kept in storage following Chen et al. (2022). Half of these leaf samples were prepared for scanning electron microscope (SEM) images, while the other half were used for the analysis of water-soluble inorganic ions and the determination of leaf functional traits.

2.3. Quantitative analysis of deposited particles

2.3.1. Number density of particles

Six 1 cm × 1 cm fragments were randomly cut from each leaf sample for analysis. These fragments were divided into two halves, with one half used to examine the adaxial surface, and the other half used to examine the abaxial surface. These fragments were affixed to the sample chamber of an SEM using conductive adhesive. The surfaces of the leaf samples were then coated with gold by an ion sputter coater (SBC-12, KYKY, China) for 40 s. Then, SEM (Phenom XL, Phenom-World, the Netherlands) coupled with an energy dispersion X-ray spectrometer (EDS), were used to acquire images of five randomly selected spots per fragment in a low vacuum mode (15 kV), with a magnification of ×

2000.

The SEM images were analyzed with ImageJ software-FIJI project (National Institutes of Health, USA) to determine the number density and size distribution of particles retained on the adaxial and abaxial surfaces of tree leaves, and elemental compositions of the major particle types were obtained by SEM-EDS. The particles were classified into fine particles ($\Phi \leq 2.5$ μm), coarse particles ($2.5 < \Phi \leq 10$ μm) and large particles ($\Phi > 10$ μm) based on particle sizes, as well as the total suspended particulate (TSP), which was the sum of all particles retained on leaf surfaces. The particle density (10^2 mm^{-2}) was calculated as follows:

$$\text{Particle density} = \frac{\text{Particle number}}{\text{SEM image area}} \tag{1}$$

2.3.2. Mass concentration of particles

The particle mass concentration per unit leaf area (μg cm^{-2}) was calculated by the following equations:

$$V_i = \frac{4}{3}\pi\left(\frac{D}{2}\right)^3 \tag{2}$$

$$\text{Particle mass} = \frac{\sum_i V_i \bullet \rho}{\text{SEM image area}} \tag{3}$$

where.

V_i is the corresponding particle volume;

D is the corresponding particle equivalent spherical diameter;

ρ is the average density of particles, and the value is 2 μg cm^{-3} here.

2.3.3. Mass concentration of water-soluble inorganic ions

The leaf samples were submerged in centrifuge tubes containing 50 mL of deionized water, and were then placed in a shaker and agitated at 30 r min^{-1} for 1 h. Subsequently, these leaves were redried in an oven at 60 °C to constant weight, while the sample solution was filtered using a 10 mL syringe equipped with a 2.2 μm filter. The resulting filtrate was injected into an ion chromatograph (Dionex ICS-600, Thermo Fisher Scientific) to determine the measured value of the major water-soluble inorganic ion concentrations, such as, Ca^{2+}, NH_4^+, SO_4^{2-}, and NO_3^-. The actual concentrations of these ions (W_i, μg cm^{-2}) were calculated as follows:

$$W_i = \frac{C_i \bullet V_s}{LA} \tag{4}$$

where.

C_i is the measured value of the water-soluble inorganic ion concentration;

V_s is the volume of the sample solution;

LA is the leaf area of the leaf sample.

2.4. Measurements of leaf functional traits

2.4.1. Morphological characteristics of tree leaves

Images of the leaf samples were obtained with an EPSONV700 scanner (Seiko Epson, Nagano, Japan) and were measured for leaf area (LA, cm^2) using WinFOLIA (Regent Instruments Inc., Quebec, Canada).

2.4.2. Photosynthetic traits

Photosynthetic traits were measured on the labeled leaves before sample collection. Photosynthesis rate, stomatal conductance, and transpiration rate, were measured using the LICOR 6400 photosynthesis system (Li-6400). Chlorophyll *a*/b was measured using a SPAD 502 plus chlorophyll meter (KONICA MINOLTA, Japan). For each species treatment, 10 labeled leaves were selected for measuring photosynthetic traits, with three replications.

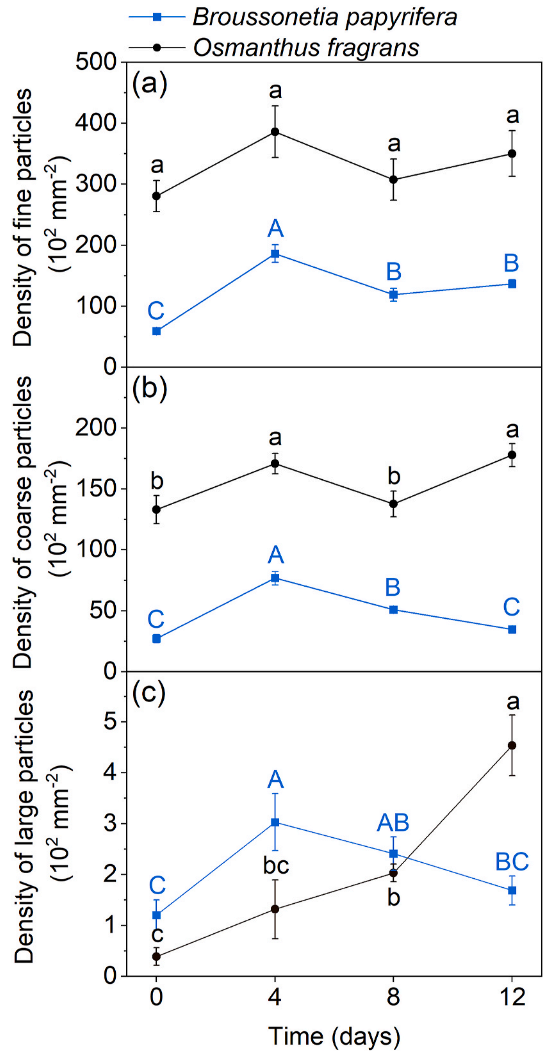

Fig. 1. Number densities of fine particles ($\Phi \leq 2.5$ μm) (a), coarse particles ($2.5 < \Phi \leq 10$ μm) (b), and large particles ($\Phi > 10$ μm) (c) on the leaves of *B. papyrifera* (blue line) and *O. fragrans* (black line). The data are presented as the mean ± SE (n = 10). Different letters indicate significant differences. (For interpretation of the references to colour in this figure legend, the reader is referred to the Web version of this article.)

2.4.3. Cuticular wax content

The redried leaves in Section 2.3 were weighed, and the measurements were recorded as m_1 (mg). Leaf samples were completely soaked in trichloromethane for 3 min before they were placed in the oven until the organic solvent was completely evaporated. Finally, the samples were reweighed, and the measurements were recorded as m_2 (mg). The wax content (WC, μg cm^{-2}) was calculated by the following equation:

$$WC = \frac{m_1 - m_2}{LA} \tag{5}$$

where.

m_1 is the dry weight of the leaf sample;

m_2 is the dry weight with wax removal;

LA is the leaf area of the leaf sample.

2.5. Data analyses

The data were analyzed using SPSS 26.0 statistical software (SPSS Inc., Chicago, IL, USA), and the charts were mainly created with Origin 2021 software (OriginLab Corp., Northampton, MA, USA). Specifically,

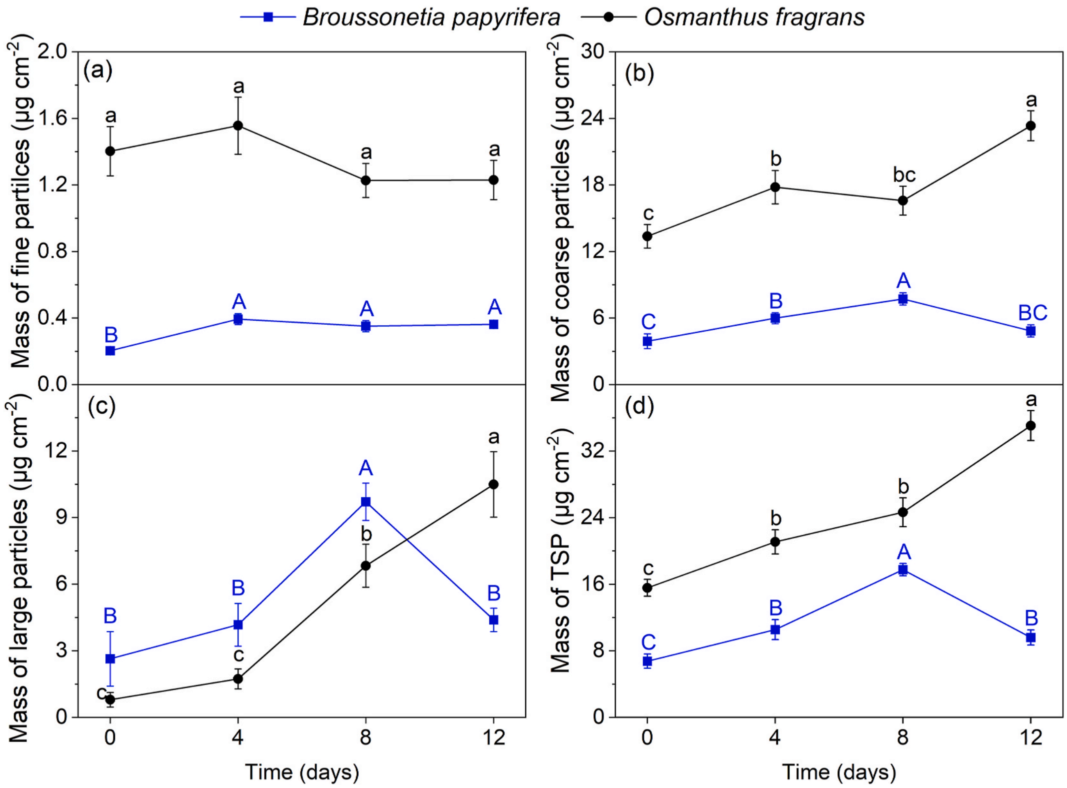

Fig. 2. Mass concentrations of fine particles (a), coarse particles (b), large particles (c), and total suspended particulates (TSP) (d), retained on the leaves of *B. papyrifera* (blue line) and *O. fragrans* (black line). The data are presented as the mean ± SE (n = 10). Different letters indicate significant differences. (For interpretation of the references to colour in this figure legend, the reader is referred to the Web version of this article.)

two-way analysis of variance (two-way ANOVA) and Duncan's multiple comparison were employed to illustrate the differences in the particle characteristics and leaf functional traits of the deposited trees. In addition, principal component analysis (PCA) was adopted to investigate the major compositions and possible sources of aerosol particles deposited on leaf surfaces, and Pearson correlation analysis was conducted to demonstrate the correlations between the particle characteristics and leaf functional traits.

3. Results

3.1. Dynamic changes in the retained particles of different sizes

Both the accumulation period and plant species had significant effects on the number densities of fine and coarse particles, except for fine particles deposited on *O. fragrans* (Fig. 1), whereas the number density of large particles was mainly affected by the accumulation period (Table S1). The number densities of deposited particles increased quickly at the beginning, with maximum values occurring on the fourth day. Then, the particle accumulation on *B. papyrifera* leaves decreased over the accumulation periods. In contrast, the deposition of large particles on the *O. fragrans* leaves consistently increased over time, while the fine and coarse particles exhibited fluctuations (Fig. 1). *O. fragrans* was more efficient than *B. papyrifera* in retaining fine and coarse particles, while more large particles were retained on *O. fragrans* than on *B. papyrifera* on the 12th day.

Over time, the mass concentrations of the different-sized particles retained on *B. papyrifera* and *O. fragrans* leaves exhibited difference (Fig. 2). The accumulation period and plant species were major factors to influence the mass concentrations of the coarse particles and TSP (Table S1). However, mass concentrations of fine particles retained on the leaves were significantly affected by plant species, whereas concentrations of large particles were mainly influenced by the accumulation periods (Table S1). Compared with *B. papyrifera*, *O. fragrans* was more efficient at retaining fine particles, coarse particles, and TSP. In general, mass concentration of fine particles did not change significantly during the accumulation periods. However, mass concentration of coarse particles and large particles retained on *B. papyrifera* leaves peaked on the eighth day, while mass concentration of coarse particles and large particles retained on the *O. fragrans* leaves continued to increase even on the 12th day (Fig. 2).

High-resolution SEM images coupled with EDS revealed significant differences in leaf microstructures and deposited particles between the adaxial and abaxial surfaces of the *B. papyrifera* and *O. fragrans* leaves (Fig. 3). The leaves of *B. papyrifera* with wrinkles and grooves were covered with dense trichomes and scattered with closed stomata. The adaxial surfaces of the *B. papyrifera* leaves exhibited numerous wrinkles and grooves, while the abaxial surfaces were covered with dense trichomes and had scattered closed stomata. The adaxial surface of the *O. fragrans* leaves was glabrous with a cuticular wax layer, and the abaxial surface was filled with opening stomata. On the other hand, the particle deposition on *B. papyrifera* increased and peaked on the eighth day before it decreased, while that on *O. fragrans* increased consistently with the accumulation period. *B. papyrifera* and *O. fragrans* both exhibited similar phenomenon that more particles deposited on the adaxial leaves than on the abaxial leaves, and the abaxial leaves tended to retain large particles in a similar change trend as the adaxial leaves (Fig. 3).

The particles deposited on plant leaves had different compositions (Fig. 4). For example, spherical metal particles with smooth surfaces generally contained metal elements, such as Fe and Ba (Fig. 4a and b). In most cases, irregular mineral particles with rough surfaces were found to contain elements such as O, Ca, Si, and Al (Fig. 4c–f). Additionally, numerous secondary particles originating from various and complex sources were observed on the adaxial and abaxial surfaces (Fig. 4d–f, h). Interestingly, a few fungal spores and hyphae were detected on the

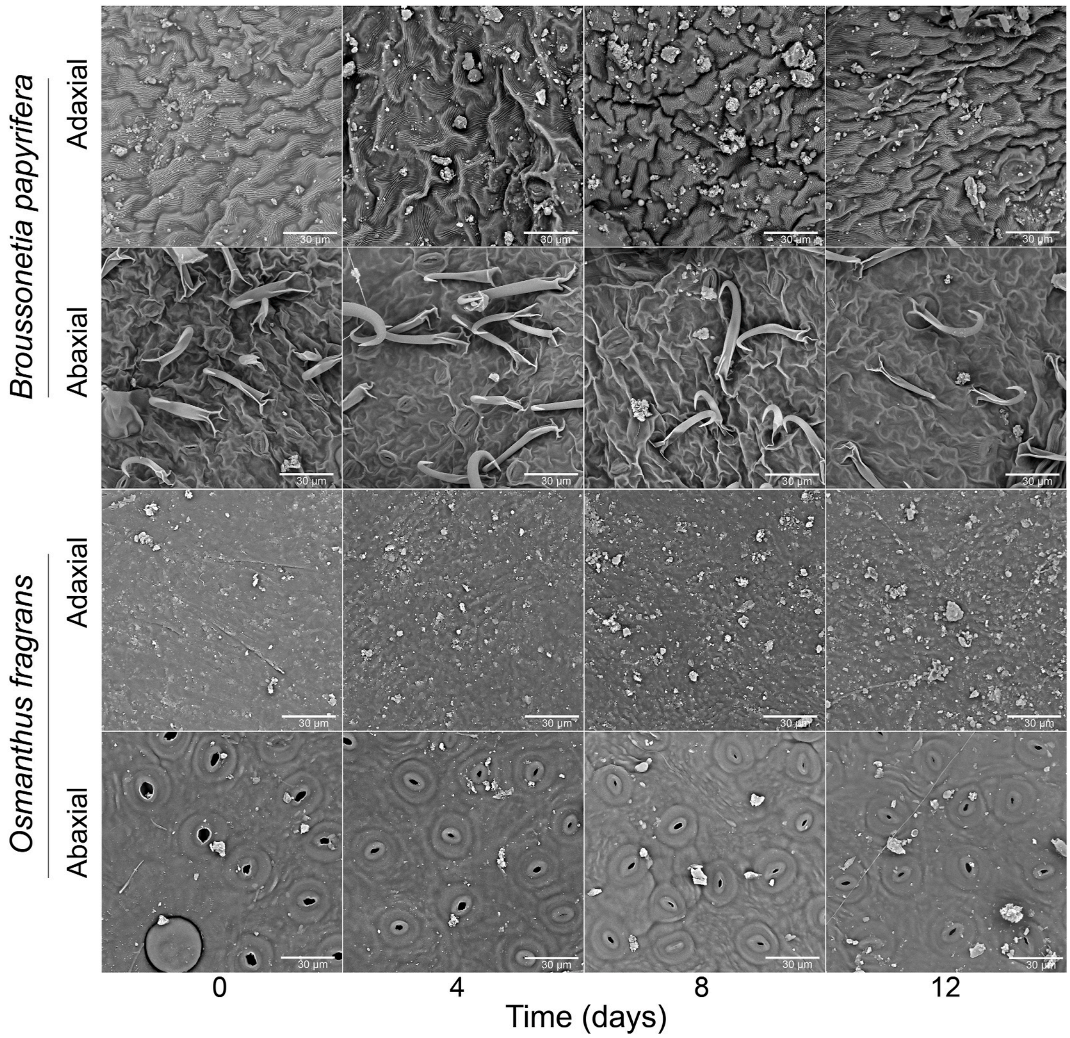

Fig. 3. Scanning electron microscopy (SEM) images of the aerosol particles retained on the adaxial and abaxial leaf surfaces of *B. papyrifera* and *O. fragrans* (× 2000 magnification) with accumulation for 0 day, 4 days, 8 days, and 12 days.

abaxial surfaces of plant leaves (Fig. 4g and h).

The concentrations of water-soluble inorganic ions in the deposited particles varied with accumulation periods and plant species (Fig. 5). The increased concentrations of Ca^{2+} and NO_3^- were significantly influenced by accumulation period, plant species, and their interactions, whereas the concentrations of NH_4^+ and SO_4^{2-} were affected by accumulation period, respectively (Table S1, Fig. 5). For particles on *B. papyrifera*, the concentrations of Ca^{2+}, SO_4^{2-} and NO_3^- had similar trends as those from *O. fragrans*, while concentration of NH_4^+ displayed an opposite trend (Fig. 5). Fig. 5 shows that *O. fragrans* took higher concentrations of Ca^{2+} and SO_4^{2-} but lower concentration of NO_3^-, compared with *B. papyrifera*.

The PCA tool was used to determine the characteristics of the particles retained on the leaves of *B. papyrifera*, and *O. fragrans* (Fig. 6). The first principal component (PC1) (*i.e.*, Ca^{2+} and SO_4^{2-}) explained 49.6% of the total variability in the fine particles, coarse particles, TSP. These components mainly represented PM retained on the *O. fragrans* leaves. The second principal component (PC2) shows that NO_3^- had a positive correlation with large particles. It explained 24.5% of all factors that described the characteristics of the particles retained on *B. papyrifera* leaves.

3.2. Impacts of deposited particles on leaf functional traits

Leaf functional traits exhibited different trends with accumulation period and plant species (Table S2). Specifically, the photosynthesis rate, chlorophyll *a*/b and wax content were significantly affected by the accumulation period and plant species. The transpiration rate was influenced by the accumulation period, plant species, and their interactions, while stomatal conductance was solely affected by the accumulation period (Table S2).

The functional traits of the plant leaves responded differently to accumulation period, but their trends were similar between *B. papyrifera* and *O. fragrans,* except for wax content (Fig. 7). With increasing time of particulate accumulation, chlorophyll *a*/b initially increased and then decreased in *B. papyrifera* and *O. fragrans*, reaching a peak on the 4th day, while the photosynthesis rate consistently decreased. The trends of stomatal conductance and transpiration rate reflected the photosynthesis rate. The wax content of the *B. papyrifera* leaves followed a similar trend of chlorophyll *a*/b (Fig. 7). Interestingly, the wax content of the *O. fragrans* leaves was 10–30 times higher than that of *B. papyrifera* leaves. The wax content of the *O. fragrans* firstly decreased on the 4th day and then increased consistently (Fig. 7f). In contrast, the wax content of *B. papyrifera* increased and peaked on the 4th day of accumulation and then decreased consistently.

Correlation analysis was conducted between the leaf functional traits and mass concentrations of the retained particles on *B. papyrifera* and *O. fragrans* (Fig. 8). The mass concentrations of TSP retained on *B. papyrifera* and *O. fragrans* were positively correlated with large and coarse particles, suggesting that retained particles mainly originated

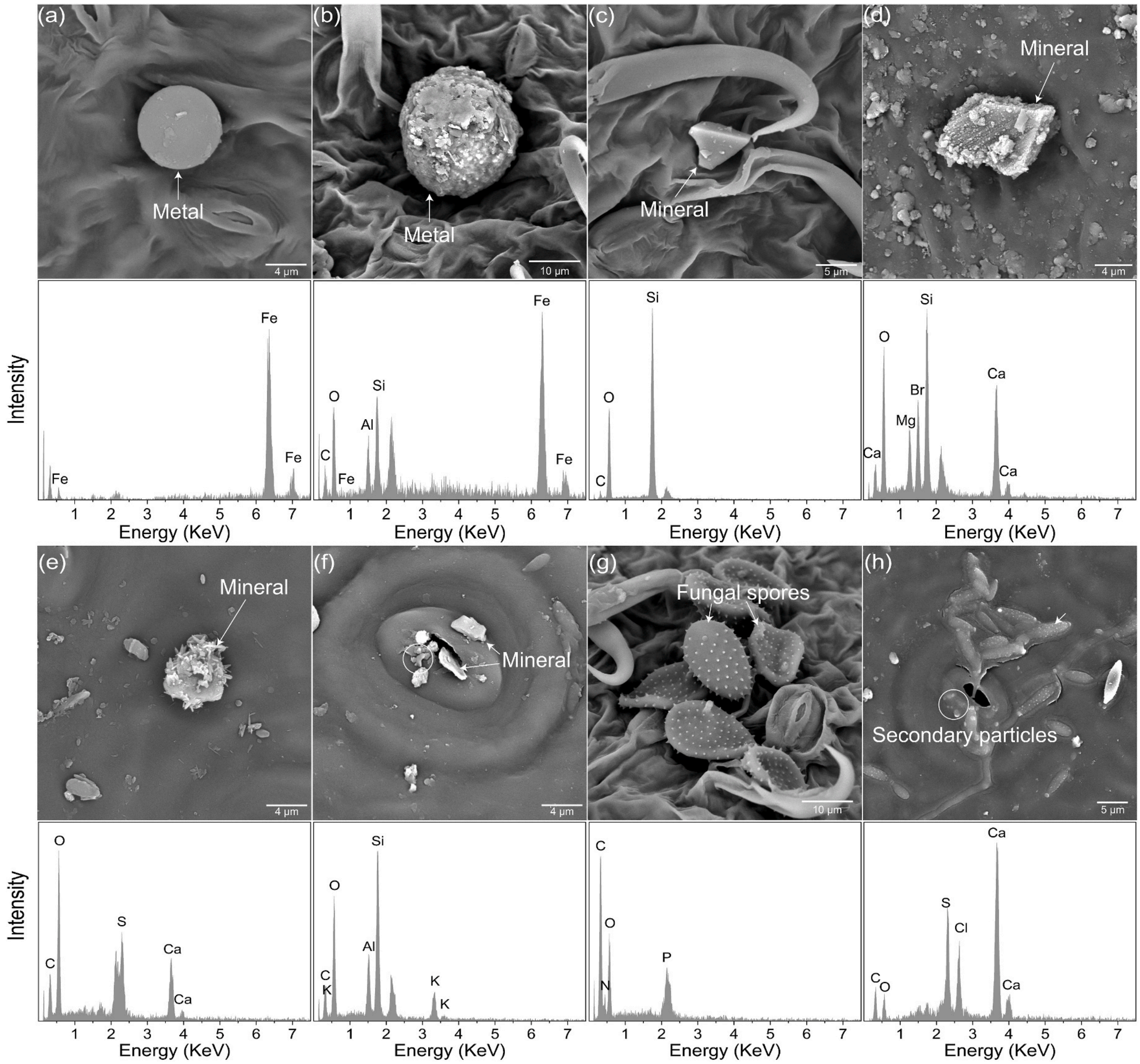

Fig. 4. High-resolution SEM images coupled with EDS (SEM-EDS) for the different types of particles on the leaf surfaces, such as, spherical metal (Fe) particles from a steel factory (a), mineral particles attached to spherical metal particles (b), mineral particles (c), secondary aerosol particles densely aggregated on the foliar surface (d), mineral and secondary aerosol particles (e), mineral and secondary aerosol particles existing inside and outside of a stoma (f), biological particles (*i.e.*, fungal spores) (g), and secondary aerosol particles and biological particles (*i.e.*, fungal hyphae and spores) embedded in the cuticular wax of the plant leaves (h).

from large and coarse particles. The mass concentrations of coarse particles, large particles, and TSP were negatively correlated with the photosynthesis rate and chlorophyll *a*/b (Fig. 8). These differences existed in the correlations between leaf functional traits and particle mass of the tree species. Specifically, the wax content of *O. fragrans* was positively correlated with the mass concentrations of the coarse particles, large particles and TSP, while the wax content of *B. papyrifera* was negatively correlated with the mass concentrations of the large particles and TSP. The mass concentration of the coarse particles on *B. papyrifera* was negatively correlated with the stomatal conductance and transpiration rate, while the mass concentrations of the coarse particles, large particles and TSP on *O. fragrans* were positively correlated with the stomatal conductance and transpiration rate.

4. Discussion

Many studies indicated that vegetation can reduce the concentrations of aerosol particles and improve air quality (Fares et al., 2020; Nemitz et al., 2020). In this study, the number densities and mass concentrations of the different-sized particles retained on the leaves of deciduous *B. papyrifera* and evergreen *O. fragrans* exhibited different changes following the particle accumulation period increased. The number densities of the particles retained on the *B. papyrifera* leaves reached saturation on the 4th day, while the mass concentrations of the particles peaked on the 8th day (Figs. 1–3). This result possibly caused by the coagulation of fine particles agglomerating together to form larger particles (Yin et al., 2020). As the different trend shown in Fig. 1, the mass concentrations of the particles on *O. fragrans* continued to increase even on the 12th day. Therefore, evergreen and deciduous plants had different accumulation mechanisms of aerosol particles. For instance, Sun et al. (2018) reported that the accumulation of particles on six shrubs peaked approximately 24 days after rainfall; Wang et al. (2015) demonstrated that PM on new leaf surfaces of three deciduous species reached a high amount within 4–7 days at a high PM level. These results show that plant species with different growth forms and leaf surface features likely take different time to achieve saturation in particle retention due to their different physiological functions and leaf functional traits.

Previous studies considered particle accumulation on plant leaves through filtration weighing and their possible sources based on water-

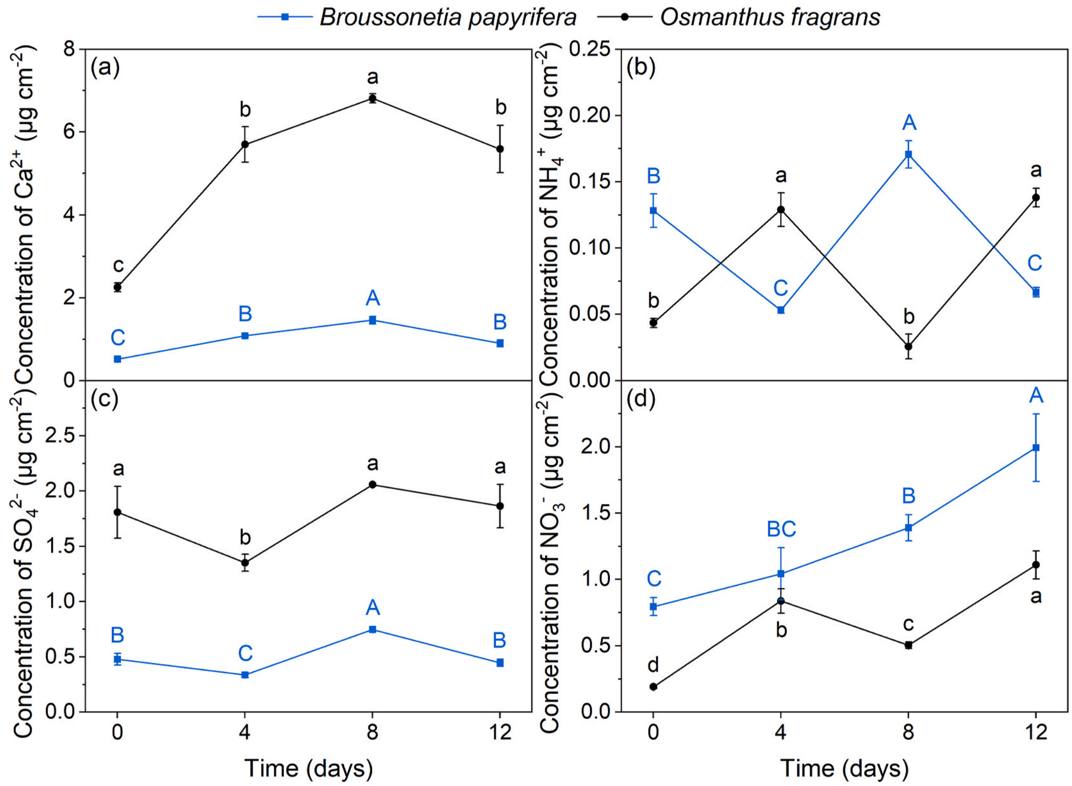

Fig. 5. Mass concentrations of water-soluble ions, including Ca^{2+} (a), NH_4^+ (b), SO_4^{2-} (c), and NO_3^- (d) of the total suspended particles (TSP) retained on the leaves of *B. papyrifera* (blue line) and *O. fragrans* (black line). The data are presented as the mean ± SE (n = 10). Different letters indicate significant differences. (For interpretation of the references to colour in this figure legend, the reader is referred to the Web version of this article.)

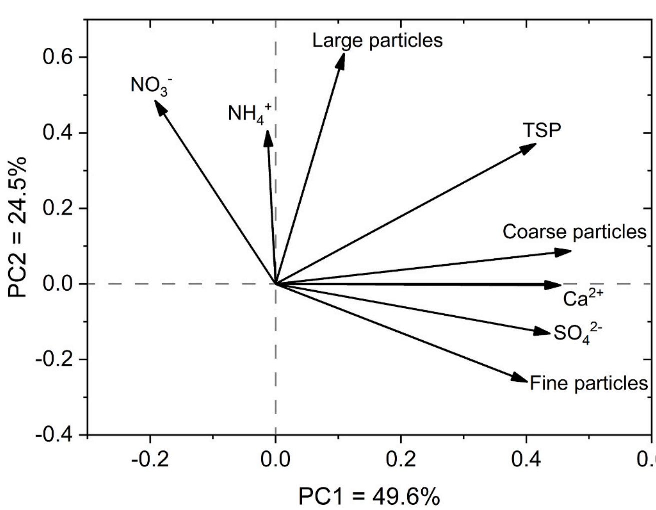

Fig. 6. Principal components analysis (PCA) on the mass concentrations of particles with different sizes (*i.e.*, fine particles, coarse particles, large particles, and total suspended particulates (TSP)), and the mass concentrations of water-soluble ions (*i.e.*, NH_4^+, Ca^{2+}, SO_4^{2-}, and NO_3^-), retained on the leaf surfaces of plants, responding to the accumulation period treatments. PC indicates a principal component.

soluble inorganic ions deposited on plant leaves (Konczak et al., 2021; Li et al., 2021). In this study, Ca^{2+}, SO_4^{2-} and NO_3^- were the dominant water-soluble inorganic ions on the leaves of *B. papyrifera* and *O. fragrans*. The result is consistent with the data reported by Xu et al. (2018) who reported that Ca^{2+}, SO_4^{2-} and NO_3^- were the major components of particles retained on the urban trees in Beijing. However, the leaking out of water-soluble inorganic ions from plant leaves cannot be neglected. For example, Chen et al. (2022) found that K^+ with high concentration was leaked from leaf tissue during sample treatment. In this study, to prevent leaking of soluble ions, we adopted soft operations and kept one good leaf without damages. Indeed, we did not detect K^+ in the most particle samples, suggesting no obvious ion leaching during the experimental process. Generally, Ca^{2+} was considered to source from resuspended and construction dust, while SO_4^{2-}, NO_3^- and NH_4^+ were sourced from secondary inorganic particles by gas-to-particle reactions (*e.g.*, NO_2, SO_2 and NH_3). Surprisingly, we found little NH_4^+ in the deposited particles. The reason can be possibly attributed to the ions absorption (*e.g.*, NH_4^+, NO_3^-, and SO_4^{2-}) by plants as foliar fertilizers (Gao et al., 2020; Moale et al., 2021).

Particle deposition is closely related to the growth forms and leaf functional traits of plants (Barwise and Kumar, 2020; Corada et al., 2021). Compared to *B. papyrifera*, the *O. fragrans* leaves had a higher wax content and retained more atmospheric particles (Fig. 7), particularly fine and coarse particles. The result shows that evergreen *O. fragrans* was more efficient in particle retention than deciduous *B. papyrifera*. This finding is consistent with the statement that the wax content of plant leaves is helpful for particle accumulation (Chen et al., 2022). Moreover, the wax content of the *O. fragrans* leaves increased with accumulation period, suggesting that it is an acclimation mechanism to particle stresses (Popek et al., 2018). In contrast, we found that the particles retained on the *B. papyrifera* leaves caused the degradation of cuticular wax (Fig. 7), which is consistent with the study by Konczak et al. (2021). The opposite result likely attributed to the rate of wax synthesis being lower than that of degradation due to the low growth stage in winter. Rough and densely covered with trichomes on the leaf surface (Fig. 2) facilitated the retention of larger particles (Prigioniero et al., 2022; Weerakkody et al., 2017), suggesting that cuticular wax and trichomes of *B. papyrifera* leaf trichomes contribute to particle accumulation.

Environmental stress, such as soil nutrient deficiency, deficit and

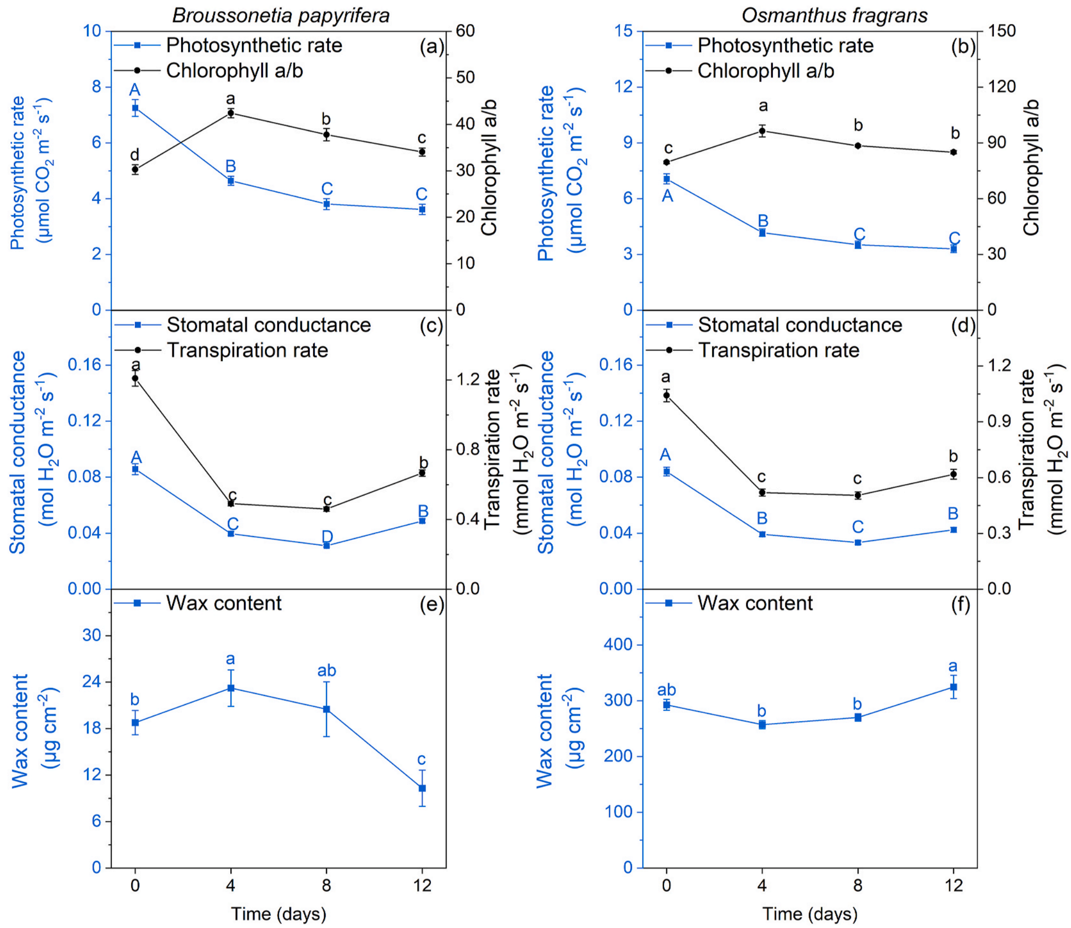

Fig. 7. Photosynthetic rates and chlorophyll *a/b* (a, b), stomatal conductance and transpiration rates (c, d), and wax contents (e, f) of *B. papyrifera* and *O. fragrans* respectively. The data are presented as the mean ± SE (n = 10). Different letters indicate significant differences.

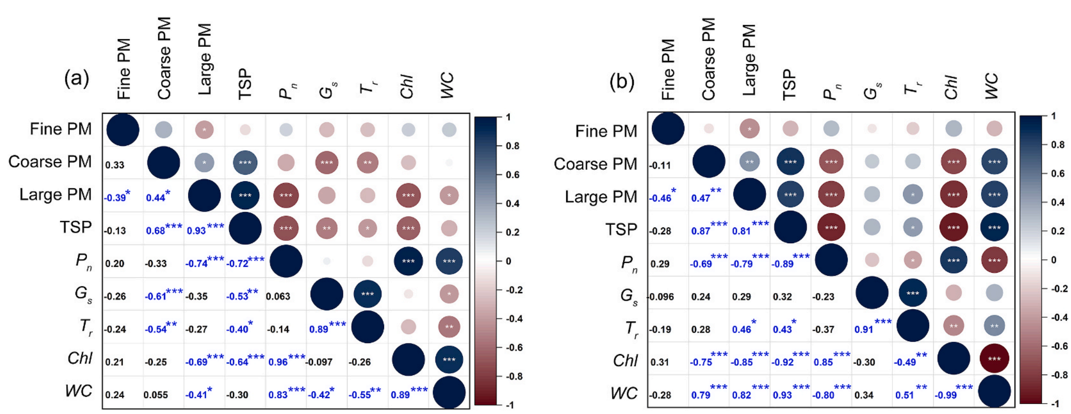

Fig. 8. Correlation analysis of particle masses of different sizes (*i.e.*, fine particles, coarse particles, large particles, and total suspended particulates (TSP)) and the leaf functional traits (*e.g.*, photosynthetic rate (P_n), stomatal conductance (G_s), transpiration rate (T_r), chlorophyll *a*/b (*Chl*), and wax content (*WC*)) of *B. papyrifera* (a) and *O. fragrans* (b). * - $p < 0.05$, ** - $p < 0.01$, *** - $p < 0.001$.

contamination of water, and limited sunlight, can affect plant photosynthesis (Chaves et al., 2009; Liu et al., 2022). However, few studies have investigated the impacts of particle accumulation on plants. In this study, particle accumulation exhibited significantly negative effects on the photosynthesis rate and chlorophyll *a*/b, which decreased during the accumulation period and negatively affected by particle accumulation. The similar result, a decreasing rate of photosynthesis due to the presence of PM accumulated on foliage, have been reported by Popek et al. (2018). Recently, Huang et al. (2023) indicated that chlorophyll was degraded by automobile exhaust pollution. It is noted that plant photosynthesis is greatly influenced by many factors, such as light intensity, temperature, CO_2 concentration, and season conditions. The definite answer remains unclear how PM plays a major role in the decrease in photosynthesis and chlorophyll. Therefore, further studies are needed to explore the effects of PM on plant photosynthesis.

The adverse effects of aerosol particles on plant leaves can not be ignored. Fine particles can enter the interior of a leaf through the open stomata and damage foliar internal tissues, causing various physiological changes, such as symptoms of chlorosis, premature aging, and necrosis of leaves (Siqueira-Silva et al., 2016). In this study, we found that the retention of coarse or large particles on plant leaves clog stomata (Fig. 4), resulting in reduced stomatal conductance and transpiration rate as well as photosynthesis rate (Popek et al., 2018). Moreover, these particles contained heavy metals, polycyclic aromatic hydrocarbons, and other toxic components, which cause leaf injury, stomata damage, and a reduction in photosynthetic activity, and further reduce the productivity and functionality of trees (Konczak et al., 2021; Weerakkody et al., 2018). Simultaneously, particle pollution could stimulate urban trees to emit a considerable amount of different compounds, known as biogenic volatile organic compounds (BVOCs) (Siqueira-Silva et al., 2016). The mechanisms and potential effects underlying the interactions between particle accumulation and plant responses warrant further investigation.

5. Conclusions

The leaf functional traits of plant species were closely related to particle retention efficiency, especially the cuticular wax of plant leaves, which significantly contributed to particle accumulation. Compared with *B. papyrifera*, the leaves of *O. fragrans* had higher wax content and retained more atmospheric particles, particularly fine and coarse particles, suggesting that evergreen *O. fragrans* was more efficient at particle retention than deciduous *B. papyrifera*. We found that the number densities and mass concentrations of the retained particles tended to decrease following reaching saturation. The particle accumulation efficiency of different plant species varied with their growth forms and leaf surface features.

Particle accumulation exhibited adverse effects on the functional traits of plant leaves, resulting in the decrease of photosynthesis and chlorophyll of plants during the accumulation periods, and potentially reducing their productivity and functionality. The retention of coarse or large particles on plant leaves can clog stomata, reducing stomatal conductance and transpiration rate. The water-soluble inorganic ions (*e.g.*, NH_4^+, SO_4^{2-}, and NO_3^-) in secondary aerosol particles might be nutritious. However, the toxic components of retained particles (*e.g.*, heavy metals, polycyclic and aromatic hydrocarbons) potentially had leaf injury and stomatal damage, and finally increased wax content as an acclimation mechanism to particle stress. Therefore, the acclimation mechanisms of plants in response to particle stresses should be investigated in the future.

Author statement

Siqi Chen and Hua Yu: Funding acquisition, Conceptualization, Methodology, Investigation, Software, Data curation, Writing-original draft, and Writing-review & editing. Liang Xu and Fangmin Fei: Investigation, Methodology. Yaobin Song and Ming Dong: Writing-review & editing. Weijun Li: Resources, Writing-review.

Declaration of competing interest

The authors declare that they have no known competing financial interests or personal relationships that could have appeared to influence the work reported in this paper.

Data availability

Data will be made available on request.

Acknowledgements

This project was funded by the National Natural Science Foundation of China (31700475).

Appendix A. Supplementary data

Supplementary data to this article can be found online at https://doi.org/10.1016/j.envpol.2023.122812.

References

Alves, C.A., Evtyugina, M., Vicente, A.M.P., Vicente, E.D., Nunes, T.V., Silva, P.M.A., Duarte, M.A.C., Pio, C.A., Amato, F., Querol, X., 2018. Chemical profiling of PM(10) from urban road dust. Sci. Total Environ. 634, 41–51. https://doi.org/10.1016/j.scitotenv.2018.03.338.

Baldacchini, C., Castanheiro, A., Maghakyan, N., Sgrigna, G., Verhelst, J., Alonso, R., Amorim, J.H., Bellan, P., Bojovic, D.D., Breuste, J., Buhler, O., Cantar, I.C., Carinanos, P., Carriero, G., Churkina, G., Dinca, L., Esposito, R., Gawronski, S.W., Kern, M., Le Thiec, D., Moretti, M., Ningal, T., Rantzoudi, E.C., Sinjur, I., Stojanova, B., Anicic Urosevic, M., Velikova, V., Zivojinovic, I., Sahakyan, L., Calfapietra, C., Samson, R., 2017. How does the amount and composition of PM deposited on Platanus acerifolia leaves change across different cities in Europe? Environ. Sci. Technol. 51, 1147–1156. https://doi.org/10.1021/acs.est.6b04052.

Banerjee, S., Banerjee, A., Palit, D., 2022. Morphological and biochemical study of plant species- a quick tool for assessing the impact of air pollution. J. Clean. Prod. 339, 130647 https://doi.org/10.1016/j.jclepro.2022.130647.

Barwise, Y., Kumar, P., 2020. Designing vegetation barriers for urban air pollution abatement: a practical review for appropriate plant species selection. npj Clim. Atmos. Sci. 3, 12. https://doi.org/10.1038/s41612-020-0115-3.

Beckett, K.P., Freer-Smith, P.H., Taylor, G., 2000. Particulate pollution capture by urban trees: effect of species and windspeed. Global Change Biol. 6, 995–1003. https://doi.org/10.1046/j.1365-2486.2000.00376.x.

Burkhardt, J., Pariyar, S., 2014. Particulate pollutants are capable to 'degrade' epicuticular waxes and to decrease the drought tolerance of Scots pine (Pinus sylvestris L.). Environ. Pollut. 184, 659–667. https://doi.org/10.1016/j.envpol.2013.04.041.

Cao, Z., Wu, X., Wang, T., Zhao, Y., Zhao, Y., Wang, D., Chang, Y., Wei, Y., Yan, G., Fan, Y., Yue, C., Duan, J., Xi, B., 2022. Characteristics of airborne particles retained on conifer needles across China in winter and preliminary evaluation of the capacity of trees in haze mitigation. Sci. Total Environ. 806, 150704 https://doi.org/10.1016/j.scitotenv.2021.150704.

Chaves, M.M., Flexas, J., Pinheiro, C., 2009. Photosynthesis under drought and salt stress: regulation mechanisms from whole plant to cell. Ann. Bot. 103, 551–560. https://doi.org/10.1093/aob/mcn125.

Chen, S., Yu, H., Teng, X., Dong, M., Li, W., 2022. Composition and size of retained aerosol particles on urban plants: insights into related factors and potential impacts. Sci. Total Environ. 853, 158656 https://doi.org/10.1016/j.scitotenv.2022.158656.

Corada, K., Woodward, H., Alaraj, H., Collins, C.M., de Nazelle, A., 2021. A systematic review of the leaf traits considered to contribute to removal of airborne particulate matter pollution in urban areas. Environ. Pollut. 269, 116104 https://doi.org/10.1016/j.envpol.2020.116104.

Fares, S., Conte, A., Alivernini, A., Chianucci, F., Grotti, M., Zappitelli, I., Petrella, F., Corona, P., 2020. Testing removal of carbon dioxide, ozone, and atmospheric particles by urban parks in Italy. Environ. Sci. Technol. 54, 14910–14922. https://doi.org/10.1021/acs.est.0c04740.

Gao, P.P., Xue, P.Y., Dong, J.W., Zhang, X.M., Sun, H.X., Geng, L.P., Luo, S.X., Zhao, J.J., Liu, W.J., 2021. Contribution of PM(2.5)-Pb in atmospheric fallout to Pb accumulation in Chinese cabbage leaves via stomata. J. Hazard Mater. 407, 124356 https://doi.org/10.1016/j.jhazmat.2020.124356.

Gao, P.P., Zhang, X.M., Xue, P.Y., Dong, J.W., Dong, Y., Zhao, Q.L., Geng, L.P., Lu, Y., Zhao, J.J., Liu, W.J., 2022. Mechanism of Pb accumulation in Chinese cabbage leaves: stomata and trichomes regulate foliar uptake of Pb in atmospheric PM(2.5). Environ. Pollut. 293, 118585 https://doi.org/10.1016/j.envpol.2021.118585.

Gao, Y., Chen, C., Wang, D., Zhang, L., Cai, D., Wu, Z., 2020. TiO2/Biochar with light-switchable wettability as a herbicide safener and foliar fertilizer adhesive. ACS Sustain. Chem. Eng. 8, 1121–1128. https://doi.org/10.1021/acssuschemeng.9b06047.

Grantz, D.A., Garner, J.H., Johnson, D.W., 2003. Ecological effects of particulate matter. Environ. Int. 29, 213–239. https://doi.org/10.1016/S0160-4120(02)00181-2.

He, C., Qiu, K.Y., Alahmad, A., Pott, R., 2020. Particulate matter capturing capacity of roadside evergreen vegetation during the winter season. Urban For. Urban Green. 48, 126510 https://doi.org/10.1016/j.ufug.2019.126510.

Health Effects Institute, 2020. State of Global Air 2020. Special Report. Health Effects Institute, Boston, MA.

Huang, H., He, Z., Li, M., Zhou, Y., Zhang, J., Jin, X., Chen, J., 2023. Influence of exposure history on the particle retention capacity and physiological responses of Euonymus japonicus Thunb. var. aurea-marginatus Hort. Environ. Pollut. 316, 120593 https://doi.org/10.1016/j.envpol.2022.120593.

Janhäll, S., 2015. Review on urban vegetation and particle air pollution – deposition and dispersion. Atmos. Environ. 105, 130–137. https://doi.org/10.1016/j.atmosenv.2015.01.052.

Konczak, B., Cempa, M., Pierzchala, L., Deska, M., 2021. Assessment of the ability of roadside vegetation to remove particulate matter from the urban air. Environ. Pollut. 268, 115465 https://doi.org/10.1016/j.envpol.2020.115465.

Li, W., Xu, L., Liu, X., Zhang, J., Lin, Y., Yao, X., Gao, H., Zhang, D., Chen, J., Wang, W., Harrison, R.M., Zhang, X., Shao, L., Fu, P., Nenes, A., Shi, Z., 2017. Air pollution-aerosol interactions produce more bioavailable iron for ocean ecosystems. Sci. Adv. 3, e1601749 https://doi.org/10.1126/sciadv.1601749.

Li, X., Zhang, T., Sun, F., Song, X., Zhang, Y., Huang, F., Yuan, C., Yu, H., Zhang, G., Qi, F., Shao, F., 2021. The relationship between particulate matter retention capacity and leaf surface micromorphology of ten tree species in Hangzhou, China. Sci. Total Environ. 771, 144812 https://doi.org/10.1016/j.scitotenv.2020.144812.

Li, Y., Wang, S., Chen, Q., 2019. Potential of thirteen urban greening plants to capture particulate matter on leaf surfaces across three levels of ambient atmospheric pollution. Int. J. Environ. Res. Publ. Health 16. https://doi.org/10.3390/ijerph16030402.

Liu, H., Xiao, C., Qiu, T., Deng, J., Cheng, H., Cong, X., Cheng, S., Rao, S., Zhang, Y., 2022. Selenium regulates antioxidant, photosynthesis, and cell permeability in plants under various abiotic stresses: a review. Plants 12, 44. https://doi.org/10.3390/plants12010044.

Lu, S.W., Yang, X.B., Li, S.N., Chen, B., Jiang, Y., Wang, D., Xu, L., 2018. Effects of plant leaf surface and different pollution levels on PM2.5 adsorption capacity. Urban For. Urban Green. 34, 64–70. https://doi.org/10.1016/j.ufug.2018.05.006.

Moale, C., Ghiurea, M., Sirbu, C.E., Somoghi, R., Cioroianu, T.M., Faraon, V.A., Lupu, C., Trica, B., Constantinescu-Aruxandei, D., Oancea, F., 2021. Effects of siliceous natural nanomaterials applied in combination with foliar fertilizers on physiology, yield and fruit quality of the apricot and peach trees. Plants 10. https://doi.org/10.3390/plants10112395.

Nemitz, E., Vieno, M., Carnell, E., Fitch, A., Steadman, C., Cryle, P., Holland, M., Morton, R.D., Hall, J., Mills, G., Hayes, F., Dickie, I., Carruthers, D., Fowler, D., Reis, S., Jones, L., 2020. Potential and limitation of air pollution mitigation by vegetation and uncertainties of deposition-based evaluations. Philos. Trans. R. Soc. A-Math. Phys. Eng. Sci. 378, 20190320 https://doi.org/10.1098/rsta.2019.0320.

Pace, R., Guidolotti, G., Baldacchini, C., Pallozzi, E., Grote, R., Nowak, D.J., Calfapietra, C., 2021. Comparing i-Tree Eco estimates of particulate matter deposition with leaf and canopy measurements in an urban Mediterranean holm oak forest. Environ. Sci. Technol. 55, 6613–6622. https://doi.org/10.1021/acs.est.0c07679.

Piscitello, A., Bianco, C., Casasso, A., Sethi, R., 2021. Non-exhaust traffic emissions: sources, characterization, and mitigation measures. Sci. Total Environ. 766, 144440 https://doi.org/10.1016/j.scitotenv.2020.144440.

Popek, R., Haynes, A., Przybysz, A., Robinson, S.A., 2019. How much does weather matter? Effects of rain and wind on PM accumulation by four species of Australian native trees. Atmosphere 10. https://doi.org/10.3390/atmos10100633.

Popek, R., Przybysz, A., Gawronska, H., Klamkowski, K., Gawronski, S.W., 2018. Impact of particulate matter accumulation on the photosynthetic apparatus of roadside woody plants growing in the urban conditions. Ecotoxicol. Environ. Saf. 163, 56–62. https://doi.org/10.1016/j.ecoenv.2018.07.051.

Prigioniero, A., Zuzolo, D., Niinemets, U., Postiglione, A., Mercurio, M., Izzo, F., Trifuoggi, M., Toscanesi, M., Scarano, P., Tartaglia, M., Sciarrillo, R., Guarino, C., 2022. Particulate matter and polycyclic aromatic hydrocarbon uptake in relation to leaf surface functional traits in Mediterranean evergreens: potentials for air phytoremediation. J. Hazard Mater. 435, 129029 https://doi.org/10.1016/j.jhazmat.2022.129029.

Qi, Y., Wei, S., Xin, T., Huang, C., Pu, Y., Ma, J., Zhang, C., Liu, Y., Lynch, I., Liu, S., 2022. Passage of exogeneous fine particles from the lung into the brain in humans and animals. Proc. Natl. Acad. Sci. U. S. A. 119, e2117083119 https://doi.org/10.1073/pnas.2117083119.

Rai, P.K., 2016. Impacts of particulate matter pollution on plants: implications for environmental biomonitoring. Ecotoxicol. Environ. Saf. 129, 120–136. https://doi.org/10.1016/j.ecoenv.2016.03.012.

Sgrigna, G., Baldacchini, C., Dreveck, S., Cheng, Z., Calfapietra, C., 2020. Relationships between air particulate matter capture efficiency and leaf traits in twelve tree species from an Italian urban-industrial environment. Sci. Total Environ. 718, 137310 https://doi.org/10.1016/j.scitotenv.2020.137310.

Siqueira-Silva, A.I., Pereira, E.G., Modolo, L.V., Lemos-Filho, J.P., Paiva, E.A., 2016. Impact of cement dust pollution on Cedrela fissilis Vell. (Meliaceae): a potential bioindicator species. Chemosphere 158, 56–65. https://doi.org/10.1016/j.chemosphere.2016.05.047.

Sun, X., Li, H., Guo, X., Sun, Y., Li, S., 2018. Capacity of six shrub species to retain atmospheric particulates with different diameters. Environ. Sci. Pollut. Res. Int. 25, 2643–2650. https://doi.org/10.1007/s11356-017-0549-2.

Targino, A.C., Coraiola, G.C., Krecl, P., 2019. Green or blue spaces? Assessment of the effectiveness and costs to mitigate the urban heat island in a Latin American city. Theor. Appl. Climatol. 136, 971–984. https://doi.org/10.1007/s00704-018-2534-1.

Wang, L., Gong, H., Liao, W., Wang, Z., 2015. Accumulation of particles on the surface of leaves during leaf expansion. Sci. Total Environ. 532, 420–434. https://doi.org/10.1016/j.scitotenv.2015.06.014.

Weerakkody, U., Dover, J.W., Mitchell, P., Reiling, K., 2017. Particulate matter pollution capture by leaves of seventeen living wall species with special reference to rail-traffic at a metropolitan station. Urban For. Urban Green. 27, 173–186. https://doi.org/10.1016/j.ufug.2017.07.005.

Weerakkody, U., Dover, J.W., Mitchell, P., Reiling, K., 2018. Quantification of the traffic-generated particulate matter capture by plant species in a living wall and evaluation of the important leaf characteristics. Sci. Total Environ. 635, 1012–1024. https://doi.org/10.1016/j.scitotenv.2018.04.106.

Xie, C., Kan, L., Guo, J., Jin, S., Li, Z., Chen, D., Li, X., Che, S., 2018. A dynamic processes study of PM retention by trees under different wind conditions. Environ. Pollut. 233, 315–322. https://doi.org/10.1016/j.envpol.2017.10.073.

Xu, X., Zhang, Z., Bao, L., Mo, L., Yu, X., Fan, D., Lun, X., 2017. Influence of rainfall duration and intensity on particulate matter removal from plant leaves. Sci. Total Environ. 609, 11–16. https://doi.org/10.1016/j.scitotenv.2017.07.141.

Xu, Y., Xu, W., Mo, L., Heal, M.R., Xu, X., Yu, X., 2018. Quantifying particulate matter accumulated on leaves by 17 species of urban trees in Beijing, China. Environ. Sci. Pollut. Res. Int. 25, 12545–12556. https://doi.org/10.1007/s11356-018-1478-4.

Yin, S., Lyu, J., Zhang, X., Han, Y., Zhu, Y., Sun, N., Sun, W., Liu, C., 2020. Coagulation effect of aero submicron particles on plant leaves: measuring methods and potential mechanisms. Environ. Pollut. 257, 113611 https://doi.org/10.1016/j.envpol.2019.113611.

Yuan, Q., Qi, B., Hu, D., Wang, J., Zhang, J., Yang, H., Zhang, S., Liu, L., Xu, L., Li, W., 2021. Spatiotemporal variations and reduction of air pollutants during the COVID-19 pandemic in a megacity of Yangtze River Delta in China. Sci. Total Environ. 751, 141820 https://doi.org/10.1016/j.scitotenv.2020.141820.

Zhang, L., Zhang, Z.Q., Chen, L.X., McNulty, S., 2019. An investigation on the leaf accumulation-removal efficiency of atmospheric particulate matter for five urban plant species under different rainfall regimes. Atmos. Environ. 208, 123–132. https://doi.org/10.1016/j.atmosenv.2019.04.010.

Zhang, X., Lyu, J., Zeng, Y., Sun, N., Liu, C., Yin, S., 2021. Individual effects of trichomes and leaf morphology on PM(2.5) dry deposition velocity: a variable-control approach using species from the same family or genus. Environ. Pollut. 272, 116385 https://doi.org/10.1016/j.envpol.2020.116385.

Zhou, S., Yan, G., Wu, Y., Zhai, J., Cong, L., Zhang, Z., 2020. The PM removal process of wetland plant leaves with different rainfall intensities and duration. J. Environ. Manag. 275, 111239 https://doi.org/10.1016/j.jenvman.2020.111239.